Dense-BiGRU: Densely Connected Bi-directional Gated Recurrent Unit based Heart Failure Detection using ECG Signal

Vinitha V., V. Parthasarathy, R. Santhosh
Research scholar, Department of Computer Science and Engineering, Faculty of Engineering, Karpagam Academy of Higher Education, Coimbatore, Tamil Nadu, India
[2]Dean, R&D and Industry Relations, Karpagam Academy of Higher Education
Coimbatore, Tamil Nadu, India
[3]Professor and Head, Department of Computer Science and Engineering, Faculty of Engineering, Karpagam Academy of Higher Education, Coimbatore, Tamil Nadu, India

Emails: santhoshrd@gmail.com; deanrd@kahedu.edu.in; vinitha.ph@gmail.com

Abstract

Heart failure, a state marked by the heart's inefficiency in pumping blood adequately., can lead to serious health complications and reduced quality of life. Detecting heart failure early is crucial as it allows for timely intervention and management strategies to prevent progression and improve patient outcomes. The effectiveness of integrating ECG and AI for heart failure detection stems from AI's capacity to meticulously analyze extensive ECG datasets, facilitating the early identification of nuanced cardiac irregularities and enhancing diagnostic precision. While the current research lacks sufficient accuracy and is burdened by complexity issues. To overcome this issue, we proposed a novel Densely Connected Bi-directional Gated Recurrent Unit (Dense-BiGRU) model for accurate heart failure detection. In this work, we enhanced collected ECG signal in terms of performing multiple data pre-treatment including as denoising, powerline interference and normalization utilizing Collaborative Empirical Mode Decomposition (CEMD) algorithm, Adaptive Least Mean Square (Adaptive LMS) and min-max normalization method, respectively. Here, we utilized the LiteStream_Net layer for extracting appropriate feature from pre-processed signal. Finally, based on extracted features heart failure detection is implemented through introducing Dense-BiGRU algorithm. The proposed research is implemented using MATLAB simulation tools, and its validation is conducted through various simulation metrics including accuracy, recall, precision, F1-score, and AUC. The results of the implementation demonstrate that the proposed research surpasses existing state-of-the-art methodologies.

Keywords: Heart failure detection; Dense-BiGRU (Densely connected bi-directional gated recurrent unit); ECG signal; Classification; Data Pre-treatment.

1. Introduction

Heart failure arises when the heart fails to efficiently pump blood, resulting in insufficient circulation throughout the body. This condition stems from various factors such as coronary artery disease, hypertension, or previous heart attacks. Common symptoms include shortness of breath, fatigue, leg swelling, and exercise intolerance [1]-[3]. Treatment involves symptom management, enhancing heart function, and addressing underlying causes through medications, lifestyle adjustments, and in severe cases, surgical interventions or heart transplantation. Timely detection and intervention are pivotal for managing heart failure and enhancing the quality of life for affected individuals [4]. Early

Doi : https://doi.org/10.54216/JCIM.140204
Received: January 09, 2024 Revised: March 08, 2024 Accepted: July 01, 2024

and precise diagnosis is essential for effective management and better outcomes. Detecting heart failure promptly enables timely initiation of appropriate treatments, preventing its progression and reducing the risk of complications like cardiac arrest or stroke [5]. Furthermore, early diagnosis allows healthcare providers to implement personalized lifestyle modifications and medication regimens, optimizing symptom control and improving quality of life. Moreover, early identification of heart failure promotes patient education and empowerment, resulting in enhanced compliance with treatment regimens and better overall health results [6][7].

Electrocardiogram (ECG)-based heart failure detection offers high accuracy compared to other methods due to its direct insights into cardiac electrical activity [8]. ECG recordings detect abnormalities in heart rhythm and conduction, often indicative of underlying heart failure. This method is advantageous for its non-invasiveness and relatively low cost in assessing cardiac function. ECG findings such as arrhythmias, conduction delays, and signs of myocardial ischemia can serve as markers of heart failure [9][10]. Additionally, ECG can detect structural changes in the heart, such as left ventricular hypertrophy or atrial enlargement, common in heart failure patients. These abnormalities often precede symptomatic heart failure, enabling early detection and intervention. Compared to symptoms or imaging studies alone, ECG provides real-time, objective data aiding in accurate diagnosis. While symptoms and imaging studies are vital, they may lack specificity and correlation with heart failure severity [11]. In contrast, ECG findings directly reflect cardiac function, guiding treatment decisions. Overall, ECG-based heart failure detection is a valuable tool for clinicians, offering precise and reliable information, enhancing diagnostic accuracy, and facilitating timely intervention, ultimately improving patient outcomes [12]-[14].

Diagnosing heart failure using ECGs, though beneficial, faces several challenges. Firstly, ECGs may lack sensitivity in detecting subtle abnormalities, particularly in the early stages of heart failure or with mild symptoms [15]. Additionally, interpreting ECGs requires expertise, and variations in interpretation can lead to inconsistencies in diagnosis. Moreover, traditional ECG analysis typically involves evaluating data from a single timepoint, potentially missing transient abnormalities and dynamic changes over time. Lastly, the complexity of ECG data can hinder accurate analysis, especially in identifying nuanced patterns associated with heart failure [16]. Developing a novel Recurrent Neural Network (RNN) model presents an opportunity to address these limitations. RNNs can be trained to identify subtle patterns indicative of early-stage heart failure, thereby enhancing sensitivity in diagnosis. Furthermore, these models can automate ECG interpretation, providing consistent and reliable analyses regardless of clinician expertise [17]-[19]. By analyzing continuous ECG data, RNNs can detect dynamic changes associated with evolving heart failure, overcoming the limitation of single timepoint assessment. Additionally, RNNs excel in processing sequential data, enabling more nuanced analysis and improved detection of complex patterns associated with heart failure. Through these capabilities, novel RNN models have the potential to transform ECG-based heart failure diagnosis, leading to more accurate and timely detection and ultimately improving patient outcomes [20]. To alleviate those issues, in our work we designed novel algorithm named as Dense-BiGRU for performing accurate heart failure detection. In this work, we introduced several novel contributions to achieve accurate and effective heart failure diagnosis which are detailed as,

Introduction of a novel Dense-BiGRU model: We propose a unique architecture, the Densely Connected Bi-directional Gated Recurrent Unit (Dense-BiGRU) model, specifically designed for accurate heart failure detection. This model leverages the bidirectional nature of GRU units and dense connections to enhance feature extraction and capture temporal dependencies in ECG signals effectively. Advanced pre-processing techniques: Our work introduces sophisticated pre-processing methods to enhance the quality of collected ECG signals. This includes denoising to remove unwanted noise, mitigating powerline interference, and normalization using the Collaborative Empirical Mode Decomposition (CEMD) algorithm, Adaptive Least Mean Square (Adaptive LMS) algorithm, and min-max normalization method, respectively. These techniques ensure that the input data is optimized for subsequent analysis, improving the robustness and reliability of our heart failure detection system.

Utilization of LiteStream_Net layer for feature extraction: We employ the LiteStream_Net layer to extract relevant features from the preprocessed ECG signals. This layer is specifically designed to capture informative patterns and representations from complex data, enabling more accurate characterization of cardiac abnormalities. By incorporating this feature extraction step, we enhance the discriminative power of our model, facilitating more precise and reliable heart failure detection.

Doi : https://doi.org/10.54216/JCIM.140204
Received: January 09, 2024 Revised: March 08, 2024 Accepted: July 01, 2024

2. Literature Survey

In this section, we have reviewed state-of-arts of heart failure detection. Moreover, this section is divided into two sub-sections which are defined as follows,

A. DL-based Heart Failure Detection

Karthick et al. [21] proposed the DLECG-CVD model, a deep learning (DL)-based 1D ECG signal recognition system for diagnosing cardiovascular diseases. The process involves several steps: pre-processing, feature extraction utilizing a Deep Belief Network (DBN), hyperparameter tuning with Improved Swallow Swarm Optimization (ISSO), and classification using XG Boost. The model's performance is validated using the PTB-XL dataset. Zhang Yue et al. [22] enhanced cardiovascular disease diagnosis accuracy by incorporating DenseNet-inspired concepts into their CHF detection model. They also curated a diverse CHF database on PhysioBank and introduced an evaluation method based on "inter-patient pattern" to improve algorithm reliability. Their technique holds promise for real-time patient monitoring via portable devices. Botros et al. [23] proposed two methods for automated heart failure identification from ECG signals. Both methods utilize convolutional neural networks (CNNs), with the second model integrating an SVM layer for classification refinement. Utilizing 2-second ECG segments and datasets like MIT-BIH and BIDMC, these models enhance accuracy in heart failure detection. Daydulo Y et al. [24] suggested a DL approach for cardiac arrhythmia detection, focusing on representing temporal frequency in ECG signals. Their model efficiently categorizes ECG signals into three classes: ARR, CHF, and NSR, employing fine-tuned pre-trained models like ReSNet 50 and AlexNet. Ram et al. [25] introduced a unique hybrid DL model for cardiac arrhythmia detection, integrating three deep models—MLP, DBN, and RBM. RBM is utilized for feature extraction, DBN for classification, and MLP for hyperparameter optimization. Training and validation are conducted using MIT-BIH and PTB-ECG datasets, demonstrating robustness via high F1-Score and AUC values compared to existing models.

Wang et al. [26] put forward a hierarchical deep learning (DL) framework with a Generative Adversarial Network (GAN) to automate cardiac diagnosis from ECG signals. Their framework comprises two levels: MadeGAN at the first level distinguishes abnormal signals from ECG signals to detect anomalies, while the second level focuses on robust multi-classification for detecting various arrhythmias. Evaluation was conducted using real-world medical data from the MIT-BIH arrhythmias database. Subasi et al. [27] introduced a novel one-dimensional hexadecimal pattern for extracting meaningful features from ECG signals, incorporating Tower graph decomposition and HLABP feature extraction. Tower graph decomposition enhances classification capability using pooling methods and graph theory, with feature selection through RFINCA. Their model was compared with state-of-the-art methods. Kumar et al. [28] proposed a DL and fuzzy clustering-based approach for arrhythmia detection from ECG signals. They denoised collected signals, segmented them, and performed data augmentation to counter class imbalance effects. CNN feature extraction and fuzzy clustering classification were employed, with extensive experimentation on benchmark datasets for performance assessment. Ahmed et al. [29] introduced a novel DL 1D-CNN for classifying cardiac arrhythmias using MIT-BIH dataset, addressing class imbalance with a class weight approach. Despite this, data imbalance persists, with the evaluation conducted using various metrics including accuracy, precision, recall, F1-score average, and AUC-ROC. Rawi et al. [30] proposed the classification of 27 heart abnormalities using 12-lead ECG signals with combined DL techniques. Their end-to-end method utilizes multivariate time series data for feature representation and spatial relations among deep features. They collected a dataset from standard ECG recordings from multiple sources to generalize and alleviate data divergence, suggesting a solution to the imbalanced dataset problem.

B. Machine Learning based Heart Failure Detection

Padmaja et al. [31] proposed a machine learning-based method for predicting heart disorders. Various techniques including logistic regression, random forest, support vector machine (SVM), Gaussian naïve Bayes, gradient boosting, K-nearest neighbors, multinomial naïve Bayes, and decision trees are employed to construct classification algorithms for prediction. These classifiers are trained and tested on Cleveland data, with important characteristics selected from the input dataset through a feature selection process. Suhail et al. [32] developed an automated method for detecting heart disease using ECG analysis and symptom-based identification. This method utilizes a nonlinear vector decomposed neural network and a discrete wavelet transformer to forecast heart illness. Preprocessing involves training a nonlinear vector to determine the presence or absence of heart illnesses and employing the discrete wavelet transform to eliminate unwanted noise. Emir et al. [33] proposed a classification approach integrating temporal, morphological, and statistical methods for heart disease detection. A hybrid feature is obtained through correlation and regression, and a backpropagation neural network (BPNN) is utilized for classification. Other machine learning techniques such as K-

Doi : https://doi.org/10.54216/JCIM.140204
Received: January 09, 2024 Revised: March 08, 2024 Accepted: July 01, 2024

nearest neighbor (KNN), decision tree (DT), and random forest (RF) are also compared, demonstrating how merging feature extraction methods enhances both conventional machine learning approaches and the BPNN model. Hossain et al. [34] utilized five machine learning techniques—SVM, logistic regression, K-nearest neighbor, naïve Bayes, and ensemble voting classifier—to predict cardiac disease. Combining five distinct ECG datasets enhances accuracy, ensuring early detection of cardiac illness. Boujraf et al. [35] proposed an improved random forest approach combined with the AdaBoost algorithm to forecast heart illnesses. Training and testing the model on heart disease datasets from Statlog and Cleveland show that the suggested random forest approach, when combined with AdaBoost, yields favorable results compared to using the random forest algorithm alone.

In order to expedite the processing of streaming ECG data, Abu-Alhaija et al. [36] explore the combination of machine learning methods with Internet of Things (IoT) technologies. This project is probably intended to make it easier to monitor and analyse cardiac signals in real time, which will allow for early abnormality diagnosis and timely intervention.

A lightweight ensemble network architecture designed especially for ECG-based cardiac disease detection is presented by Shin et al. [27]. The objective is to create a precise and effective model that may be used in contexts with limited resources, like remote monitoring systems or wearable technology. Using machine learning techniques, Kumar et al. [28] address the classification of various cardiac diseases from ECG data. Based on ECG readings, their research likely investigates a variety of classification methods and strategies to efficiently differentiate between different kinds of cardiac problems. Convolutional neural networks (CNNs) are being used to create an autonomous screening tool for cardiovascular illnesses, according to research by Dai et al. [29]. They most likely examine how well CNNs perform in examining various ECG signal segments or intervals to pinpoint particular heart problems. For the diagnosis of cardiac illness, Asadi et al. [30] provide a diagnostic method based on random forest swarm optimisation. Their goal is probably to use swarm intelligence approaches to improve the random forest algorithm's performance, which will increase the efficiency and accuracy of diagnosing heart illness using clinical data and ECG signals.

3. Dense-BiGRU Framework

This section offers diagrammatic and mathematical justifications for the proposed model. The architectural pipeline of the suggested Dense-BiGRU is illustrated in Fig. 1, comprising two key components: (i) Data Pre-processing for enhancing ECG signal and (ii) Dense-BiGRU based heart failure detection. Definitions for each of these procedures are provided below.

A. Data Pre-processing

Three primary pre-processing stages are carried out on signals obtained from the MIT-BIH database during the Data Pre-Processing stage: denoising, power line interference reduction and normalization. Reducing the processing load on process and convolution operations during feature extraction and processing is the main objective of this data pre-processing. The accuracy of heart failure detection is finally improved by increasing the efficiency of data pre-processing by removing undesired noises and interferences.

Doi : https://doi.org/10.54216/JCIM.140204
Received: January 09, 2024 Revised: March 08, 2024 Accepted: July 01, 2024

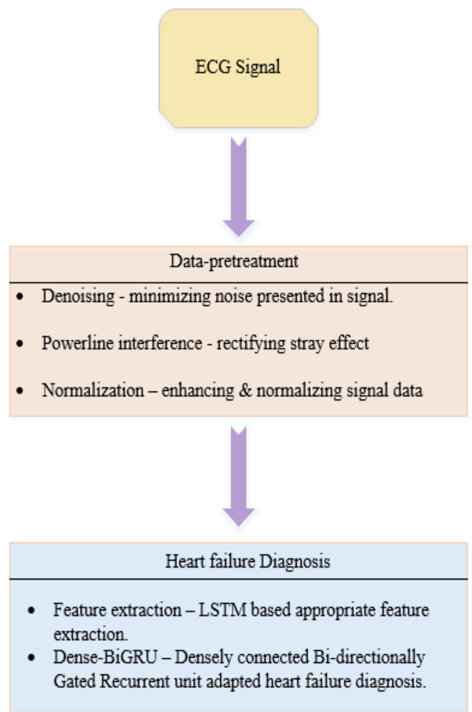

Figure 1: Architecture Pipeline

(i) ECG Signal Denoising

The proposed method advocates employing the Collaborative Empirical Mode Decomposition (CEMD) algorithm for decomposing the noisy signal into noisy Intrinsic Mode Functions (IMFs). Subsequently, a tailored modification of the thresholding function is applied to these noisy IMFs, denoted by the symbol $\mathfrak{F}_i(\mathbb{p})$. Let $\mathfrak{s}(\mathbb{p})$ represent the provided noisy signal.

$$\mathfrak{s}(\mathbb{p}) = \mathcal{O}(\mathbb{p}) + \mathcal{F}(\mathbb{p})$$

$\mathcal{F}(\mathbb{p})$ represents independent noise with finite amplitude, while $\mathcal{O}(\mathbb{p})$ represents the noiseless signal. The steps entailed in the proposed CEMD-Custom approach are outlined below:

To isolate the noisy Intrinsic Mode Functions (IMFs), decompose the noisy signal utilizing the CEMD method.

For the noisy IMFs, apply a modified custom thresholding function $\mathfrak{F}_i(\mathbb{p})$. To devise a new one, adapt the customized thresholding function in the following manner:

$$\hat{\mathcal{Y}}(\mathbb{p}) = \begin{cases} \mathfrak{F}_i(\mathbb{p}) - \mathrm{sign}\big(\mathfrak{F}_i(\mathbb{p})\big)[1-\beta]_{\sigma_i}, & \mathrm{if}|\mathfrak{F}_i(\mathbb{p})| \geq \sigma_i \\ 0 & ,\mathrm{if}|\mathfrak{F}_i(\mathbb{p})| \geq \vartheta \end{cases}$$

Here, $0 < \vartheta < \sigma_i$ & $0 \leq \beta \leq 1$ and σ_i is universal threshold.

$$\sigma_i = \mathrm{C}\sqrt{\mathcal{E}_i 2\mathbb{l}(\mathfrak{N})}$$

where $\mathfrak{N}$ represents the length of the signal, C is a constant that varies depending on the signal type, and $\mathcal{E}_i$ is determined by:

Doi : https://doi.org/10.54216/JCIM.140204
Received: January 09, 2024 Revised: March 08, 2024 Accepted: July 01, 2024

$$\mathcal{E}_i = \frac{\mathcal{E}_1^2}{\alpha}\tau^{-i}, \quad i = 1,2,3 \ldots\ldots, \mathfrak{N}$$

Here, $\mathcal{E}_1^2$ is first energy of IMF,

$$\mathcal{E}_1^2 = \left(\frac{\text{median}|\mathfrak{F}_i(\mathbb{p})|}{0.6745}\right)^2$$

Here, $\alpha = 0.719$ and $\tau = 2.01$ are constant determined empirically.

Reconstruct the signal using:

$$\hat{\mathcal{O}}(\mathbb{p}) = \sum_{i=1}^{\mathfrak{N}} \widehat{\mathcal{Y}_j}(\mathbb{p}) + \mathfrak{r}(\mathbb{p})$$

Where $\mathfrak{r}(\mathbb{p})$ denotes the residual signal. Figure 2 illustrates denoising process using CEMD.

(ii) Powerline Interference

Furthermore, we've addressed power line interferences by filtering out noise below 50Hz. To mitigate these interferences, we've employed an Adaptive Least Mean Square (Adaptive LMS) with a cut-off frequency of 50Hz. A ECG signal which has power line interference is defined as,

$$\text{ECG}_{\text{PI}}(n) = \text{Clean}_{\text{sig}}(n) + \lambda_{\text{PI}}(n)$$

Here, $\text{ECG}_{\text{PI}}(n)$ represents the ECG signal along with power line interference, $\text{Clean}_{\text{sig}}(n)$and $\lambda_{\text{PI}}(n)$ are the clean signal and power line interference. Henceforth, power line interference can be designed as sinusoidal signal which is expressed as,

$$\lambda_{\text{PI}}(n) = \Phi \sin(wn + \theta[n])$$

Where Φ denotes the maximum signal amplitude, w and θ are the frequency of power line and phase. An evaluate of sinusoidal interference is acquired through evaluating interference parameters Φ and θ. Following that, evaluated sinusoidal interference is then subtracted from leisurely ECG signal to acquire clean ECG signal. The adaptive least mean squares (LMS) method is employed for estimating the parameters Φ and θ of sinusoidal interference. Below is the residual error signal:

$$\text{er}[n] = h[n] - \lambda_{\text{PI}}(n)$$

In this scenario, the anticipated signal is denoted as $h[n]$, while the discrepancy between the expected and actual signals is represented as $\text{er}[n]$. The error observed at the nth sample and the estimations made at that sample dictate the system's parameter estimation at the subsequent (n+1) sample. Given that the phase and amplitude of the sinusoidal interference exhibit gradual changes over time, they tend to remain relatively stable within a narrow timeframe. The simplified equation for the error is as follows:

$$\text{er}[n+1] = h[n] - \lambda_{\text{PI}}(n)$$

Doi : https://doi.org/10.54216/JCIM.140204
Received: January 09, 2024 Revised: March 08, 2024 Accepted: July 01, 2024

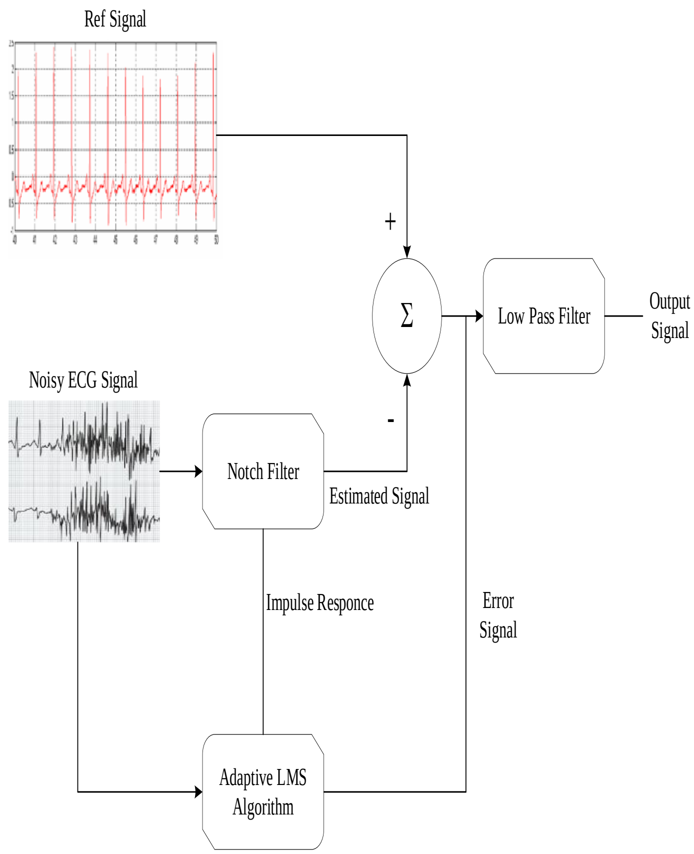

Figure 2: CEMD based Denoising

Hence, our Endeavor has been to utilize the LMS approach to minimize the mean square error, er[n]. Within the error signal er[n], both the ECG signal $\mathrm{Clean_{sig}}(n)$ and the error stemming from parameter misadjustment are encompassed. The accuracy of the interference parameter estimation is influenced by the presence of the ECG signal within the error. To refine the estimation of interference characteristics, a low-pass filter is employed to isolate the ECG signal from the erroneous signal. Given that the bulk of the energy in the ECG signal resides in the low-frequency spectrum, employing a low-pass filter effectively removes the majority of the ECG signal from the error signal. The error signal vector is subjected to low-pass filtering, and the cutoff frequency can be adjusted, ranging from above 10 Hz to 40 Hz.

(iii) Normalization

The original data is transformed linearly in this data normalization procedure. The procedure entails taking the dataset's minimum and maximum values and using the following formula to replace each value.

$$ß' = \frac{ß - \mathrm{min}(б)}{\mathrm{max}(б) - \mathrm{min}(б)}\left(\mathrm{new\_max}(б) - \mathrm{new\_min}(б)\right) + \mathrm{new\_min}(б)$$

The attribute data in this case is represented by б, and the minimum and maximum absolute values of б are indicated by the variables $\mathrm{min}(б)$ and $\mathrm{max}(б)$, respectively. Each dataset entry's initial value is denoted by ß and each entry's transformed new value is denoted by $ß'$. In addition, the intended range's maximum and lowest values are represented by $\mathrm{new\_max}(б)$ and $\mathrm{new\_min}(б)$, which act as the range's boundary values.

B. Dense-BiGRU based Heart Failure Diagnosis

Here, the LiteStreamNet layer (conv1_D1_L6) is utilized for pyramid feature extraction. Then, the significant features are selected using pyramid feature selection module where the feature maps of 128x10x8 extracted are convolved along with average kernel of 10x1. Every output of feature map as 8 illustrative features, that last become as 1024x128x8.

Doi : https://doi.org/10.54216/JCIM.140204
Received: January 09, 2024 Revised: March 08, 2024 Accepted: July 01, 2024

Furthermore, the average pooling is adapted for reducing dimensionality by acquiring the effects of overall features in kernel as its mean value. Then, the output of feature map is 1024. Following that, extracted features are fed into designed into Dense-BiGRU for further processing which are defined as,

(i) Dense-GRU

We introduce a simplified version of the Densely-connected GRU (Dense-GRU), where network blocks with dense connections incorporate skip-connections. In Fig.3, illustrating its structure, we denote the densely connected hidden unit of the l-th layer at the t-th time step as d-lt. The skip-connections between multiple levels featuring dense connections are depicted by yellow, blue, and green lines. Instead of employing the element-wise additive operation in the residual learning structure, concatenation is utilized to prevent performance degradation caused by direct gradient backpropagation.

(ii) Dense-BiGRU

A novel modeling approach is the Densely-connected Bidirectional GRU (Dense-BiGRU) network, leveraging both bidirectional features and a densely linked topology. In Dense-BiGRU, layers are interconnected not only with other layers but also with their two neighboring layers, allowing for simultaneous forward and backward data transmission. This architecture alleviates the issue of gradient vanishing, enhances feature propagation, promotes feature reuse, and significantly reduces the number of parameters. It enhances the representation of short-term temporal and spatial features. Fig. 3 illustrates how data can be transmitted both forward and backward concurrently in Dense-BiGRU. The structure comprises dual layers of GRU networks connected by densely coupled skip-connections, forming the foundation of Dense-BiGRU. These two GRU networks model the long-range temporal patterns of actions in both forward and reverse orientations. At each time step, their outputs are concatenated into a single value. The following outlines each Dense-BiGRU block:

$$\overleftrightarrow{\mathfrak{d}}_t = \vec{\mathfrak{d}}_t, \overleftarrow{\mathfrak{d}}_t$$

Here, $\overleftrightarrow{\mathfrak{d}}_t$ represents the t-th output of the Dense-BiGRU. Dense skip-connections merge the outputs of the forward and backward directions of GRU networks, where the outputs of the t-th time step are denoted as $\vec{\mathfrak{d}}_t$ and $\overleftarrow{\mathfrak{d}}_t$, respectively. The concatenation operation is symbolized by ← and →. The direction of the input sequence determines the forward and backward directions of the output denoted as $\mathfrak{d}$, respectively. The output of the l-th layer at the t-th time step, $\mathfrak{d}_t^l$, is determined by the preceding layers of the LSTM block, specified as follows.

$$\mathfrak{d}_t^l = \left[\mathfrak{Y}_t^i\left(\left[\mathfrak{d}_t^0, \mathfrak{d}_t^1, \dots, \mathfrak{d}_t^i, \dots, \mathfrak{d}_t^{l-1}\right]\right), \mathfrak{Z}_t\right]$$

From above equation, $\left[\mathfrak{d}_t^0, \mathfrak{d}_t^1, \dots, \mathfrak{d}_t^i, \dots, \mathfrak{d}_t^{l-1}\right]$ denotes the extracted features concatenation of prior module. $\mathcal{H}^1(\mathfrak{Z})$ is the l-th GRU networks. The GRU's output, reset gate output, and update gate output are denoted as $\mathfrak{K}_t$, $\mathfrak{R}_t$, and $\mathfrak{G}_t$, respectively. Moreover, the input $\mathbb{I}_t$ at the current time step and the output $\mathfrak{K}_{t-1}$ from the previous time step are jointly regulated by the reset and update gates to ascertain the current time step's output $\mathfrak{K}_t$.

$$\mathfrak{R}_t = \rho(\mathrm{wei}_{\mathfrak{R}} \,.\, [\mathfrak{K}_{t-1}, \mathbb{I}_t])$$

$$\mathfrak{G}_t = \rho(\mathrm{wei}_{\mathfrak{G}} \,.\, [\mathfrak{K}_{t-1}, \mathbb{I}_t])$$

$\mathrm{wei}_{\mathfrak{R}}$ and $\mathrm{wei}_{\mathfrak{G}}$ denote the weights for the reset and update gates, respectively. The sigmoid function, represented by ρ, is defined as $\rho(\mathbb{I}) = 1/(1+\mathbb{e}^{-\mathbb{I}})$. The calculation formula for the result $\mathfrak{K}_t$ formulated as,

$$\mathfrak{K}_t = (1 - \mathfrak{G}_t) \times \mathfrak{K}_{t-1} + \mathfrak{G}_t \times \hat{\mathfrak{K}}_t$$

At time step t, $\hat{\mathfrak{K}}_t$ represents the candidate state of the GRU. The computation for this is detailed as follows,

$$\hat{\mathfrak{K}}_t = \tan\mathfrak{K}(\mathrm{wei}_{\mathfrak{K}} . [\mathfrak{R}_t \times \mathfrak{K}_{t-1}, \mathbb{I}_t])$$

Doi : https://doi.org/10.54216/JCIM.140204
Received: January 09, 2024 Revised: March 08, 2024 Accepted: July 01, 2024

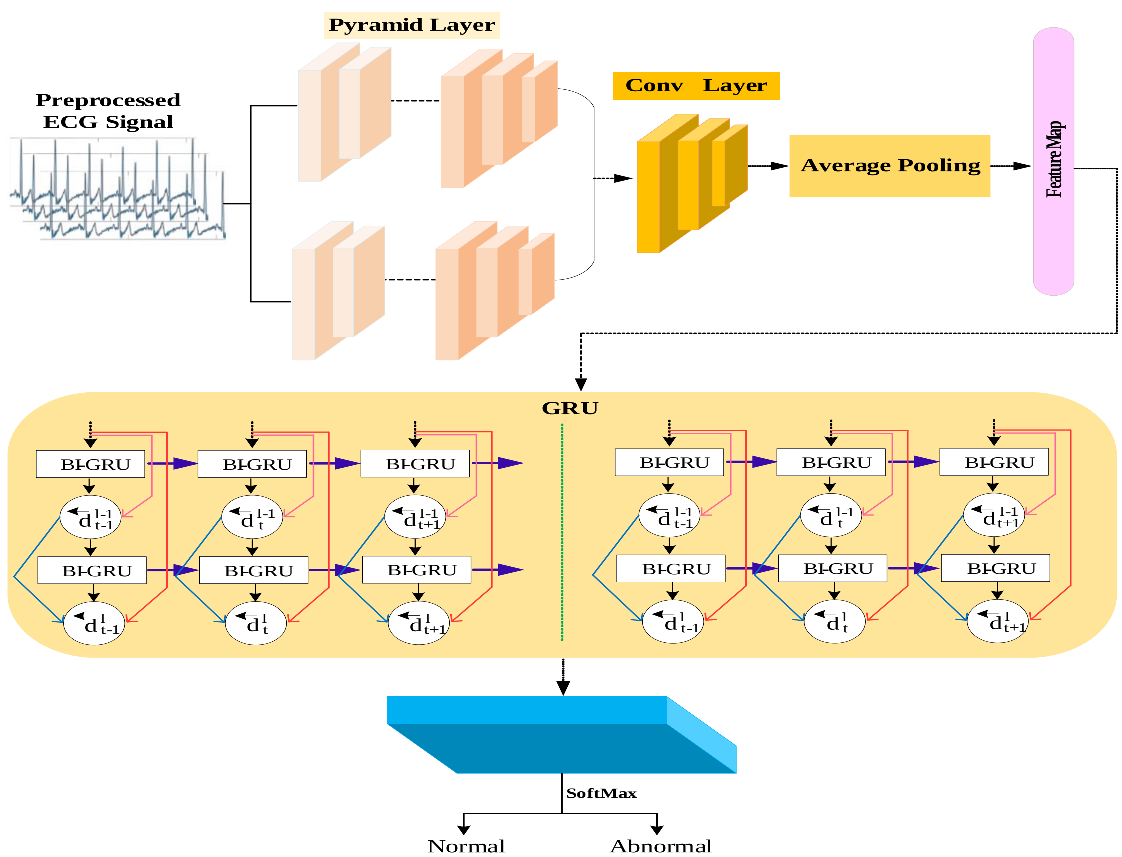

Figure 3: Proposed Dense-BiGRU based Heart Failure Detection

Here, $wei_{\mathfrak{K}}$ is the weight of the candidate state. As demonstrated earlier, two unidirectional GRUs operating in opposite directions are integrated to create the Bi-GRU (Xiong et al., 2016). The forward GRU initiates the processing of the time series data from the beginning, while the reverse GRU handles the data from the end. Utilizing two GRUs enables the computation of the Bi-GRU.

$$\overrightarrow{\mathfrak{K}}_t = \mathrm{GRU}_{\mathrm{frwd}}\left(\mathbb{I}_t, \overrightarrow{\mathfrak{K}}_{t-1}\right)$$

$$\overleftarrow{\mathfrak{K}}_t = \mathrm{GRU}_{\mathrm{bkwd}}\left(\mathbb{I}_t, \overleftarrow{\mathfrak{K}}_{t-1}\right)$$

$$\mathfrak{K}_t = \overrightarrow{\mathfrak{K}}_t \otimes \overleftarrow{\mathfrak{K}}_t$$

The state information of the forward and backward GRUs is denoted by $\overrightarrow{\mathfrak{K}}_t$ and $\overleftarrow{\mathfrak{K}}_t$ respectively. $\mathrm{GRU}_{\mathrm{frwd}}$ represents the forward GRU, while $\mathrm{GRU}_{\mathrm{bkwd}}$ signifies the backward GRU. Concatenating the $\overrightarrow{\mathfrak{K}}_t$ and $\overleftarrow{\mathfrak{K}}_t$ is illustrated by $\otimes$. Thus, traffic flow details from both past and future time series data can be retained in the Bi-GRU through the utilization of bidirectional GRU architectures.

4. Experimental Results

In this section, we explain the implementation and evaluation results of the proposed Dense-BiGRU model. The evaluation results are compared in qualitative and quantitative manner. In addition to that, we have also examined the effectiveness of the proposed model with the existing works.

A. Dataset Description

Doi : https://doi.org/10.54216/JCIM.140204
Received: January 09, 2024 Revised: March 08, 2024 Accepted: July 01, 2024

In this work, we have utilized MIT-BIH dataset which composes of ECG recording taken for 48 hours with 50 subjects among the year 1978 and 1982. There are 25 recording were randomly chosen among the 5000 set of ECG recording from the hospital of Boston berth in which 75% and 25% for the in and out patients respectively. In addition to that, there were about 480 samples/second were digitized with a range of 15mV at 12-bit resolution. Five cardiologists were manually annotated every recording in which there are about 130,0000 annotations were finally included.

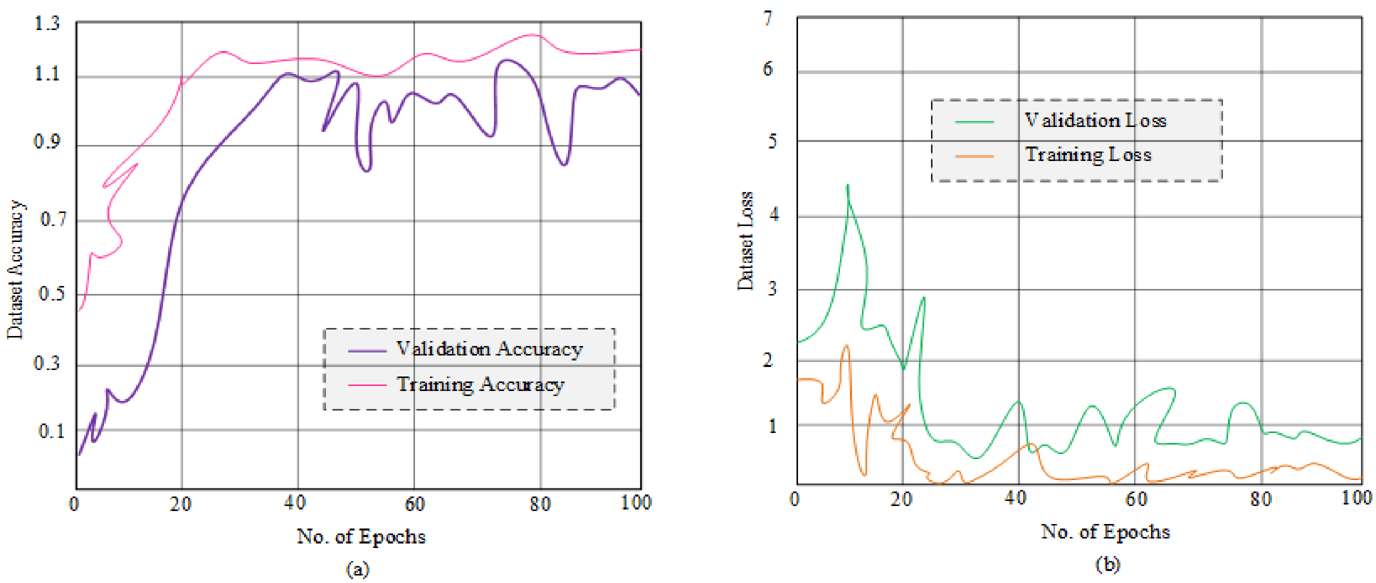

Figure 4 (a) and (b): Illustrates Performance of Accuracy and Loss

B. Implementation Details & Performance Metrics

The designed model is implemented using MATLAB simulation tool on the system with finetuned software and hardware configurations. The software configurations include Operating System (OS) of windows 11, and processor adopted was AMD Ryzen 5 5600H with Radeon Graphics 3.30 GHz. The hardware configurations comprise hard disk of 1TB with Random Access Memory (RAM) 6GB. The simulation configuration of the ECG signals are provided in table I.

Table 1: Simulation Configuration of ECG Signal

Simulation Parameter	Description	Value
Rate of Sampling	ECG signal sampling frequency	250Hz
Filtering	Filters utilized for ECG pre-processing	Discrete Wavelet Transform (DWT)
Duration of ECG signal	ECG Signal Processed Duration	15 seconds
ECG Signal	Type of	Normal

Doi : https://doi.org/10.54216/JCIM.140204
Received: January 09, 2024 Revised: March 08, 2024 Accepted: July 01, 2024

Type	ECG Signal (i.e. normal, abnormal)	rhythm, atrial fibrillation, and arrythmia
Computation of Heart Rate	Method Utilized for Computing Heart Rate	Instantaneous Heart Rate Model, and RR Average Interval
Feature Extraction	Feature Extractor Utilized for Heart Failure Detection	LSTM
Heart Failure Diagnosis	Detection Model for Heart Failure	Dense-BiGRU

In order to examine the effectiveness of the proposed model, we validating the proposed model with the existing works using various performance metrics which are listed and computed below,

$$\mathrm{F1-Score} = 2 \times \frac{\mathbb{Pr} \times \mathbb{Re}}{\mathbb{Pr} + \mathbb{Re}} \times 100$$

$$\mathrm{Rec}(\mathbb{Re}) = \frac{\mathcal{TP}}{\mathcal{TP} + \mathcal{FN}} \times 100$$

$$\mathrm{Pre}(\mathbb{Pr}) = \frac{\mathcal{TP}}{\mathcal{TP} + \mathcal{FP}} \times 100$$

$$\mathrm{Acc}(\mathfrak{A}) = \frac{\mathcal{TP} + \mathcal{TN}}{\mathcal{TP} + \mathcal{TN} + \mathcal{FP} + \mathcal{FN}} \times 100$$

From the above equation ()-(), $\mathcal{TP}$, $\mathcal{TN}$, $\mathcal{FP}$, and $\mathcal{FN}$ denotes the true positive, true negative, false positive, and false negative rates respectively. In addition to that, we have also utilized AUC-ROC curve which provides the overall assessment for the heart failure diagnosis performance. Increase the AUC-ROC performance higher the performance of the heart disease diagnosis model accuracy. Fig 4 (a) and (b) shows the analysis of accuracy and loss of the proposed model.

C. Pre-Processing Analysis

The pre-processing model utilized in the proposed work includes signal denoising using DWT, signal smoothing, and powerline interference removal using FB-LPF respectively. The adopted pre-processing models firmly removes the noise and unwanted interreference to enhance the detection accuracy and F1-score respectively. Fig 5 represents the graphical comparison of pre-processing analysis with two scenarios such as with and without pre-processing respectively. Table II denotes the quantitative performance of pre-processing process impacts towards performance metrics.

Doi : https://doi.org/10.54216/JCIM.140204
Received: January 09, 2024 Revised: March 08, 2024 Accepted: July 01, 2024

Table 2: Quantitative Performance of Pre-processing

Proposed Scenarios	Validation Metrics			
	Accuracy	Precision	Recall	F1-Score
Dense-BiGRU with Pre-Processing	98.09%	99.76%	99.26%	98.45%
Dense Bi-Gru without Pre-Processing	92.00%	92.27%	92.35%	92.89%

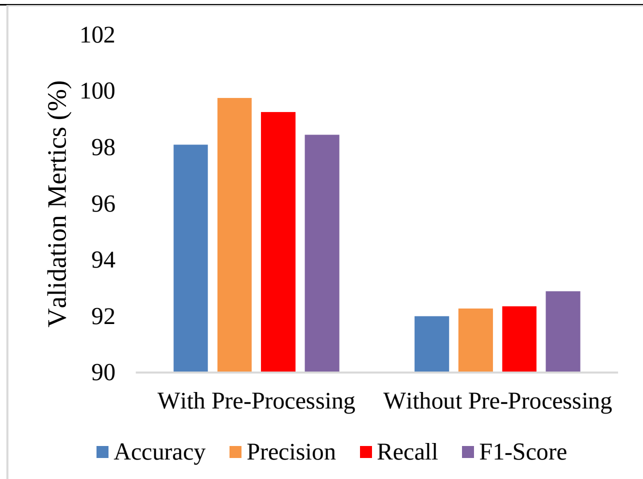

Figure 5: Comparison of With and Without Pre-processing

From the figure illustrated above, the proposed work with pre-processing process (scenario-I) gains higher validation results than proposed work without pre-processing process (scenario-II). The reason for such higher performance in the scenario-I is that, the complexity towards the model gets reduced by removing the unwanted noises, and interferences respectively. On the other hand, in scenario-II we obtain the results with higher complexity due to processing of unwanted noise and interference during model diagnosis which leads to poor validation metrics. Quantitatively, the difference of accuracy is about 6.09%, precision is about 7.49%, recall is about 6.91%, and F1-Score is about 5.56% respectively. Furthermore, we have also revealed the AUC-ROC curve which also acquires higher results than the existing works.

D. Analysis of Feature Extraction

In this section, we examine the proposed feature extractor model named Pyramidal Convolutional Feature Extractor Network (PCF-Net) with the state-of-the-art works. The state-of-the-art works includes DLECG-CVD [21], HybDeepNet [25], Fuzz-ClusterNet [28], HD-RFAB [35], and HD-LEN [37] respectively. The DLECG-CVD adopts deep belief network for feature extraction, the HybDeepNet adopts restricted botlzman machine for feature extraction, the Fuzz-ClusterNet utilized convolutional neural network for feature extraction, The HD-RFAB utilizes AdaBoost algorithm for feature extraction, and HD-LEN utilizes ensemble model for feature extraction. Table III represents the quantitative comparison of the proposed feature extraction with the existing models.

Doi : https://doi.org/10.54216/JCIM.140204
Received: January 09, 2024 Revised: March 08, 2024 Accepted: July 01, 2024

Table 3: Quantitative Performance of Feature Extraction

Existing Works	Validation Metrics			
	Accuracy	Precision	Recall	F1-Score
DLECG-CVD	85.43%	85.18%	85.24%	85.89%
HybDeepNet	87.37%	87.36%	87.43%	87.57%
Fuzz-ClusterNet	86.02%	86.85%	86.06%	86.10%
HD-RFAB	90.78%	90.18%	90.24%	90.06%
HD-LEN	94.57%	94.90%	94.93%	94.39%
Proposed (Dense-BiGRU)	99.17%	99.68%	99.36%	99.26%

Fig (6) and (7) shows the comparison of proposed Dense-BiGRU feature extraction with the state-of-the-art works. From the figure, it is shown that the proposed Dense-BiGRU achieves better feature extraction as it utilized PCG-Net for feature extraction. The pyramidal model composed of up and down convolution operations which analyses the features with granular level and provides to the convolutional correlation layers for feature map generation thereby obtaining higher feature extraction accuracy. On the other hand, the existing works mainly adopts combination of DL and ML algorithms, and also utilized ensemble models respectively feature extraction. By adopting conventional models for feature extraction, the validation accuracy of feature extraction gets diminished. Quantitatively, the difference among proposed and existing validation metrics are 4.6%-13.74%, 4.78%-14.5%, 4.43%-14.12%, and 4.87%-13.37% for accuracy, precision, recall, and F1-score respectively. On the whole, the proposed feature extractor model PCF-Net achieves higher results than the conventional models.

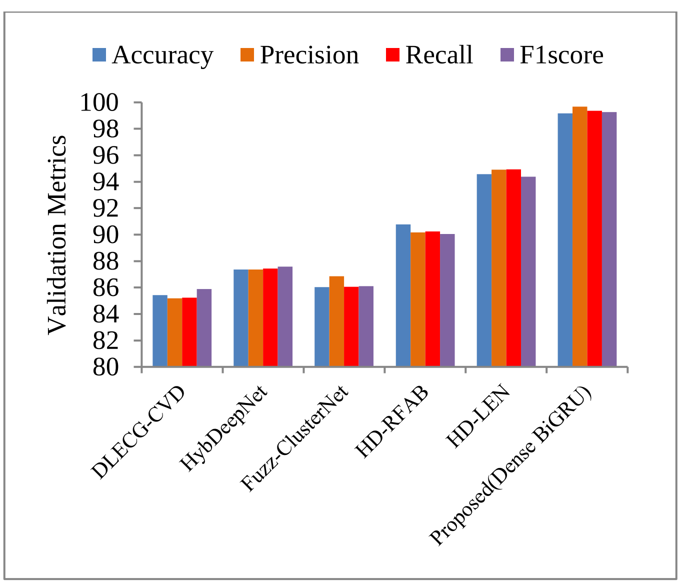

Figure 6: Comparison of Feature Extraction Performance

Doi : https://doi.org/10.54216/JCIM.140204
Received: January 09, 2024 Revised: March 08, 2024 Accepted: July 01, 2024

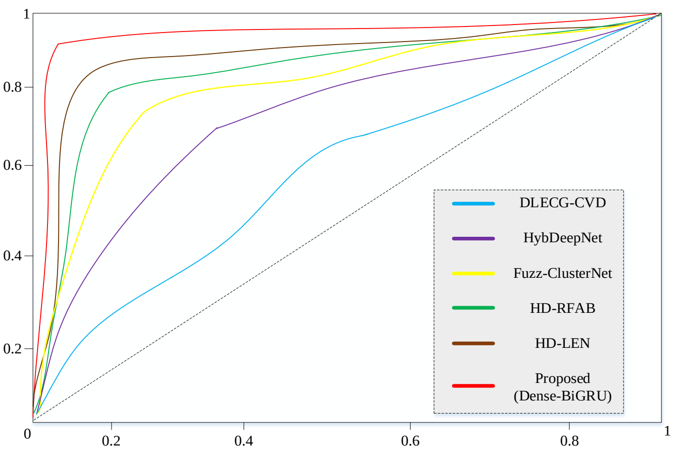

Figure 7: ROC Curve for Feature Extraction

E. Analysis of Heart Failure Diagnosis

Fig 8 shows the illustration of the heart failure detection model for the proposed Dense-BiGRU with the existing works and figure 9 represents the ROC curve. From the graphical illustration it is seen that, the proposed Dense-BiGRU achieves better detection accuracy than the state-of-the-art works. The reason for such better diagnosis accuracy is that, we adopt bidirectional processing in the GRU for capturing the long-range dependencies. Furthermore, the utilization of dense layer enables mapping of complex feature patterns among the input and output data. On the whole, the adoption of Dense-BiGRU offers flexibility, parallelism, regularization, and efficacy during heart disease diagnosis. On the other hand, the state-of-the-art works such as DLECG-CVD [21] and HybDeepNet [25] utilizes DL algorithm for heart failure diagnosis however they are lacked with underfitting issues due to lack of train data and pre-processing respectively. Whereas, the utilization of Fuzz-ClusterNet [28], HD-RFAB [35], and HD-LEN [37] adopts machine learning and clustering algorithms which lacks with interoperability issues. So that, the proposed work achieves better performance than the state-of-the-art works. From the quantitative results shown in table IV, the proposed Dense-BiGRU achieves greater diagnosis difference among the existing works which can be represented as 3.37%-16% of accuracy, 6.07%-12.91% of precision, 5.89%-14.22% of recall, and 5.66%-13.1% of F1-score respectively.

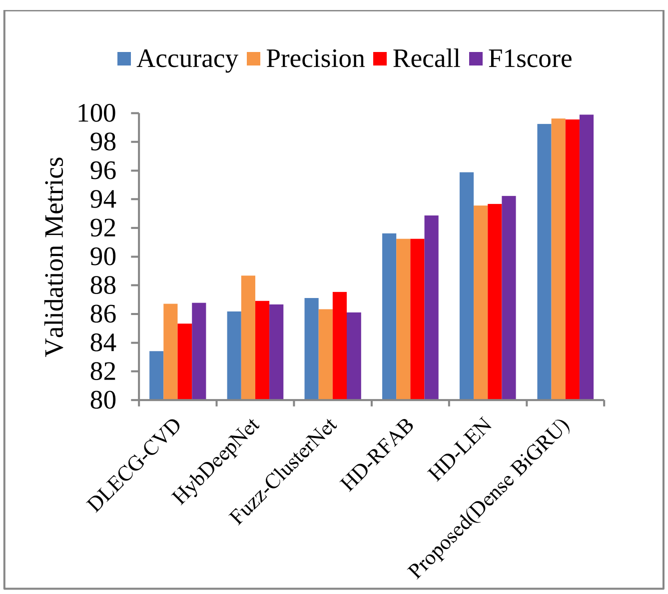

Figure 8: Performance Analysis of Heart Failure Detection

Doi : https://doi.org/10.54216/JCIM.140204
Received: January 09, 2024 Revised: March 08, 2024 Accepted: July 01, 2024

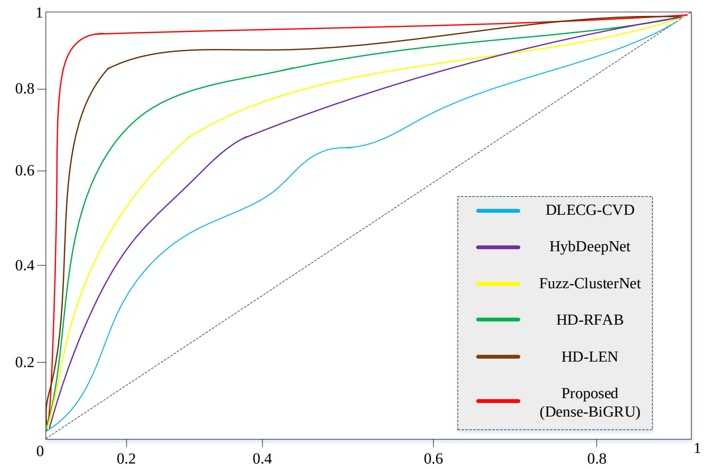

Figure 9: ROC Curve

Table 4: Performance Analysis of Proposed with Existing Models

Existing Works	Validation Metrics			
	Accuracy	Precision	Recall	F1-Score
DLECG-CVD	83.42%	86.72%	85.34%	86.78%
HybDeepNet	86.17%	88.67%	86.92%	86.67%
Fuzz-ClusterNet	87.12%	86.34%	87.54%	86.10
HD-RFAB	91.62%	91.23%	91.24%	92.23%
HD-LEN	95.87%	93.56%	93.67%	94.23%
Proposed (Dense-BiGRU)	99.24%	99.63%	99.56%	99.89%

5. Conclusion

In conclusion, the timely identification of heart failure plays a critical role in mitigating its progression and improving patient prognosis. Integrating electrocardiogram (ECG) data with artificial intelligence (AI) presents a promising avenue for refining diagnostic accuracy and precision, even amid prevailing challenges regarding data fidelity and complexity. To overcome these hurdles, we devised a novel Dense-BiGRU model, which integrates sophisticated preprocessing techniques such as denoising and normalization via Collaborative Empirical Mode Decomposition (CEMD) and Adaptive Least Mean Square (Adaptive LMS) algorithms, respectively. This framework enables the extraction of relevant features from ECG signals, enhancing the discernment of subtle cardiac irregularities. Leveraging MATLAB simulations and comprehensive validation employing diverse metrics including accuracy and F1-score, our study underscores the superiority of our proposed approach over conventional methodologies. The Dense-BiGRU model showcases remarkable efficacy in detecting heart failure, exhibiting enhanced performance and robustness in comparison to existing techniques. Our findings underscore the transformative potential of integrating AI with ECG data for augmenting heart failure detection capabilities. By offering a refined and efficient diagnostic tool, our research not only addresses the pressing need for early detection but also holds promise for improving patient care outcomes in

Doi : https://doi.org/10.54216/JCIM.140204
Received: January 09, 2024 Revised: March 08, 2024 Accepted: July 01, 2024

cardiovascular health. The demonstrated effectiveness of our Dense-BiGRU model signifies a significant advancement in the field, offering clinicians a valuable resource for timely intervention and personalized management strategies. As we continue to refine and validate our approach, the integration of AI with ECG data stands poised to revolutionize the landscape of cardiac healthcare, offering hope for enhanced patient outcomes and improved quality of life.

References

[1] Kataoka, H. (2021). Chloride in heart failure syndrome: its pathophysiologic role and therapeutic implication. Cardiology and Therapy, 10(2), 407-428.

[2] Rotz, S. J., Ryan, T. D., & Hayek, S. S. (2021). Cardiovascular disease and its management in children and adults undergoing hematopoietic stem cell transplantation. Journal of thrombosis and thrombolysis, 51, 854-869.

[3] Ambeth Kumar, V.D. (2017). Automation of Image Categorization with Most Relevant Negatives. Pattern Recognition and Image Analysis, 27(3), 371–379.

[4] Kumar, I., Kumar, A., Kumar, V.D.A. et al. (2022) Dense Tissue Pattern Characterization Using Deep Neural Network. Cogn Comput 14, 1728–1751.

[5] Shiraishi, Y., Kawana, M., Nakata, J., Sato, N., Fukuda, K., & Kohsaka, S. (2021). Time-sensitive approach in the management of acute heart failure. ESC Heart Failure, 8(1), 204-221.

[6] Ambeth Kumar, V.D. Malathi,S. Ashok Kumar. (2015). Performance Improvement Using an Automation System for Segmentation of Multiple Parametric Features Based on Human Footprint. Journal of Electrical Engineering & Technology, 10(4), 1815-1821 , 2015.

[7] Ambeth Kumar, V.D. Vaishali,S. Shweta, B. (2015). Basic Study of the Human Foot. Biomedical and Pharmacology, 8(1), 435-444.

[8] Ardeti, V. A., Kolluru, V. R., Varghese, G. T., & Patjoshi, R. K. (2023). An overview on state-of-the-art electrocardiogram signal processing methods: Traditional to AI-based approaches. Expert Systems with Applications, 217, 119561.

[9] Saini, S. K., & Gupta, R. (2022). Artificial intelligence methods for analysis of electrocardiogram signals for cardiac abnormalities: State-of-the-art and future challenges. Artificial Intelligence Review, 55(2), 1519-1565.

[10] Murat, F., Yildirim, O., Talo, M., Demir, Y., Tan, R. S., Ciaccio, E. J., & Acharya, U. R. (2021). Exploring deep features and ECG attributes to detect cardiac rhythm classes. Knowledge-Based Systems, 232, 107473.

[11] Verrier, R. L., Nearing, B. D., & D'Avila, A. (2021). Spectrum of clinical applications of interlead ECG heterogeneity assessment: From myocardial ischemia detection to sudden cardiac death risk stratification. Annals of Noninvasive Electrocardiology, 26(6), e12894.

[12] Castiglione, V., Aimo, A., Vergaro, G., Saccaro, L., Passino, C., & Emdin, M. (2022). Biomarkers for the diagnosis and management of heart failure. Heart failure reviews, 1-19.

[13] Chung, C. T., Lee, S., King, E., Liu, T., Armoundas, A. A., Bazoukis, G., & Tse, G. (2022). Clinical significance, challenges and limitations in using artificial intelligence for electrocardiography-based diagnosis. International journal of arrhythmia, 23(1), 24.

[14] Ambeth Kumar, V.D. Ramakrishnan,M. (2013). Temple and Maternity Ward Security using FPRS. Journal of Electrical Engineering & Technology, 8(3), 633-637.

[15] Kumar, V.D.A., Sharmila, S., Kumar, A. et al. (2023). A novel solution for finding postpartum haemorrhage using fuzzy neural techniques. Neural Comput & Applic. 35(33), 23683–23696

[16] Gupta, V., Mittal, M., & Mittal, V. (2021). Chaos theory and ARTFA: emerging tools for interpreting ECG signals to diagnose cardiac arrhythmias. Wireless Personal Communications, 118(4), 3615-3646.

[17] Liu, X., Wang, H., Li, Z., & Qin, L. (2021). Deep learning in ECG diagnosis: A review. Knowledge-Based Systems, 227, 107187.

[18] Sathya Preiya, V., and V. D. Ambeth Kumar. (2023). Deep Learning-Based Classification and Feature Extraction for Predicting Pathogenesis of Foot Ulcers in Patients with Diabetes. Diagnostics 13(12), 1983.

Doi : https://doi.org/10.54216/JCIM.140204
Received: January 09, 2024 Revised: March 08, 2024 Accepted: July 01, 2024

[19] Balakrishnan, Chitra, and V. D. Ambeth Kumar. (2023). IoT-Enabled Classification of Echocardiogram Images for Cardiovascular Disease Risk Prediction with Pre-Trained Recurrent Convolutional Neural Networks. Diagnostics 13(4), 775

[20] Hemamalini, Selvamani, and Visvam Devadoss Ambeth Kumar. (2022). Outlier Based Skimpy Regularization Fuzzy Clustering Algorithm for Diabetic Retinopathy Image Segmentation. Symmetry, 14(12), 2512

[21] Kavitha, D., Gnaneswar, G., Dinesh, R., Sai, Y.R., & Suraj, R. (2021). Heart Disease Prediction using Hybrid machine Learning Model. *2021 6th International Conference on Inventive Computation Technologies (ICICT)*, 1329-1333.

[22] Mohamed Suhail, M., & Abdul Razak, T. (2022). Cardiac disease detection from ECG signal using discrete wavelet transform with machine learning method. *Diabetes research and clinical practice*, 109852 .

[23] Akçin, E., İşleyen, K.S., Özcan, E., Hameed, A.A., Alimovski, E., & Jamil, A. (2021). A Hybrid Feature Extraction Method for Heart Disease Classification using ECG Signals. *2021 Innovations in Intelligent Systems and Applications Conference (ASYU)*, 1-6.

[24] Hossain, A.I., Sikder, S., Das, A., & Dey, A. (2021). Applying Machine Learning Classifiers on ECG Dataset for Predicting Heart Disease. *2021 International Conference on Automation, Control and Mechatronics for Industry 4.0 (ACMI)*, 1-6.

[25] El Hamdaoui, H., Boujraf, S., Chaoui, N.E., Alami, B., & Maaroufi, M. (2021). Improving Heart Disease Prediction Using Random Forest and AdaBoost Algorithms. *International Journal of Online and Biomedical Engineering (iJOE)*.

[26] Piyush K. Pareek, Pixel Level Image Fusion in Moving objection Detection and Tracking with Machine Learning ",Fusion: Practice and Applications, Volume 2 , Issue 1 , PP: 42-60, 2020

[27] Shivam Grover, Kshitij Sidana, Vanita Jain, "Egocentric Performance Capture: A Review", Fusion: Practice and Applications, Volume 2, Issue 2 , PP: 64-73, 2020.

[28] Abdel Nasser H. Zaied, Mahmoud Ismail and Salwa El- Sayed, A Survey on Meta-heuristic Algorithms for Global Optimization Problems, Journal of Intelligent Systems and Internet of Things, Volume 1 , Issue 1 , PP: 48-60, 2020

[29] Mahmoud H.Alnamoly, Ahmed M. Alzohairy, Ibrahim M. El-Henawy, "A survey on gel images analysis software tools, Journal of Intelligent Systems and Internet of Things, Volume 1 , Issue 1 , PP: 40-47, 2021.

[30] Sherubha, "Graph Based Event Measurement for Analyzing Distributed Anomalies in Sensor Networks", Sådhanå(Springer), 45:212, https://doi.org/10.1007/s12046-020-01451-w

Doi : https://doi.org/10.54216/JCIM.140204
Received: January 09, 2024 Revised: March 08, 2024 Accepted: July 01, 2024